

A Method for Identifying Distribution Pattern of Cone Cells in Retina Image

Ken'ichi Morooka*, Yuanting Ji*, Oscar Martinez Mozos†, Tokuo Tsuji*, Ryo Kurazume*, Peter K. Ahnelt‡

* Graduate School of Information Science and Electrical Engineering, Kyushu University

Fukuoka, Japan 819-0395, Email: see <http://fortune.ait.kyushu-u.ac.jp/about-e.html>

† School of Computer Science, University of Lincoln

Lincoln LN6 7TS, United Kingdom

‡ Dept. Neurophysiology and Neuropharmacology, Medical University of Vienna

Schwarzspanierstr. 17, A 1090, Vienna, Austria

Abstract—This paper proposes a method to identify the spatial distribution patterns of cone cells related with blood vessel in a given retina image. We define three types of the distribution patterns between cones and vessels. Positive correlation distribution (PCD) and negative correlation distribution (NCD) indicate that the cones tend to be close to or far from the vessels. While the cone cells do not have significant correlation with vessels, the cone distribution is regarded as the random distribution (RD). In our method, RD is modeled by many virtual retina images, each of which is generated by the vessels extracted from the original retina image and the virtual cells are selected randomly from the image. Using the virtual images, we estimate the distribution range of RD. When the distribution of the original cells is above the upper limit or below the lower limit of the RD distribution, the cell distribution is NCD or PCD. Otherwise, the cell distribution is regarded as RD.

I. INTRODUCTION

A Vision is one of the most important human sensors. More than 70% of all the information which our human being receives is derived from vision sensor [1]. The visual information, the lights and images, of the environment are projected onto a retina, which is basically a piece of brain tissue. The stimulations which the retina gets are captured by photoreceptor cells in the retina. There are two classic types of the photoreceptor cells; cone cells which extract color information, and rod cells which respond to the stimulation by light. The visual information received by the photoreceptor cells is converted into electrical signals, and transmitted to a human brain via optic nerves.

Technologies and materials based on the mechanism of the human vision system contribute to develop useful devices in various fields. One application is an artificial retina with a layout imitating the human eye to restore the sight to visually impaired persons [2], [3]. When robots are equipped with the vision system with a performance similar to that of the human eye, the robots will be able to work robustly in our daily environment with persons [4]. The core of developing these bio-inspired devices is to understand how the retina is designed to perform the image processing task. However, the structure of the retina and the image processing in the retina have not yet been fully understood.

Recent works [5], [6], [7], [8] have been paid attention to elucidate the structure and functions of the human vision system from an engineering point of view. Curcio et al. [6]

measured the spatial distribution of the cone cells. From their report, the peak of the cone distribution is located at around the center of the fovea, and the distribution is decreased sharply. Eglen [5] revealed the spacing between adjacent cone cells. Song et al. [7] indicated the relationship between the locations and distributions of the cone cells. In addition, their research reported that the cone distributions have been changed with aging. Recently, high-resolution retina images provided by recent microscope allow to view more details of the retina, and identify several types of biological elements constituting the retina. Using the high-resolution retina images, Mozos et al. [8] analyzed the spacial relationship between a pair of arbitrary two types of the cells. Their work suggested that the spatial relationships between elements of different types indicate possible constraints or connectivity between the different components.

This paper studies the spatial relationship between two specific elements, cone cells and vessels, in the retina using the high-resolution retina images. In our study, depending on the distance between the cells and vessels, the spatial relationship is classified into three types: positive correlation distribution(PCD), negative correlation distribution(NCD), and random distribution(RD). Given a retina image, a statistical analysis using simulation is employed to model the RD using the vessels extracted from the image. Using the model, the cone distribution in the image is identified.

II. METHOD

This section describes our method for determining the pattern of the spatial relationship between cone cells and vessels. Given a retina image, the cone cells and vessels are extracted from the retinal image, and then drawn into geometric primitives, represented by points and lines. For each cell, the minimum distance between the cell and its closest blood vessel is obtained. The spatial relationship between cone cells and vessels is represented by the curve of the cumulative frequency distribution (CFD) of the minimum distances. Using the CFD, we determine the possible spatial relationship between cone cells and vessels in the given image.

A. Extraction of cone cells and vessels

Fig. 1 shows an example of a retina image. In the figure, black points and lines are cone cells and vessels, respectively.

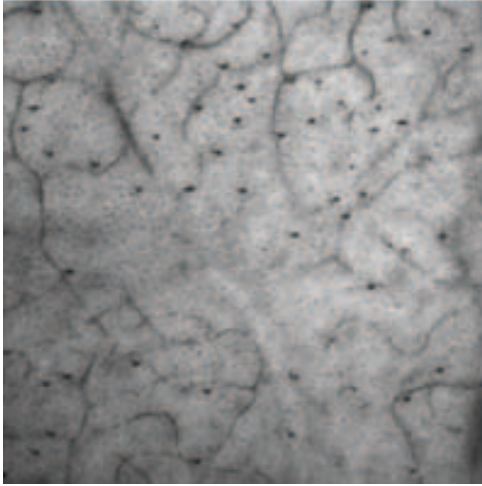


Fig. 1. Example of a retina image.

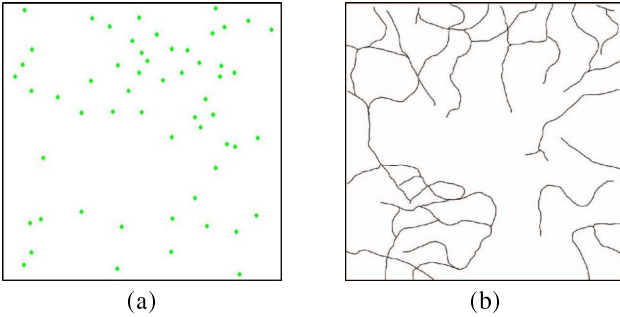


Fig. 2. Biological elements extracted from the retina image: (a)cones; (b)vessels.

These biological elements are manually extracted from the image by an experienced ophthalmologist. Thinning process is applied to the extracted vessel lines to represent the vessels with single pixel wide lines. Also, since each point extracted as the cone cell contains several pixels, each cone shrink to one pixel by morphological operation. Fig. 2(a) and (b) show the cone cells and vessels obtained by the above-described processes, and called the cone and vessel images. Here, the black pixels shown in Fig.2(b) are the vessel pixels forming the vessels.

B. Classification of cell distribution

The spatial relationship between the cells and the vessels in the image is represented by the minimum distance between the cell and the vessel. The minimum distance is calculated as the distance between the cell and its closest vessel pixel. Using the distances, called the vessel distance of the cell, a cumulative frequency distribution of the vessel distances is constructed that displays the cumulative number of the cells whose the distances is less than or equal to a specific distance. Using the CFD, the distribution of the cells is classified into three types: positive correlation distribution(PCD), negative correlation distribution(NCD), and random distribution(RD).

When the cells tend to be close to the vessels as shown in Fig.3(a), the spatial relationship between the cells and the

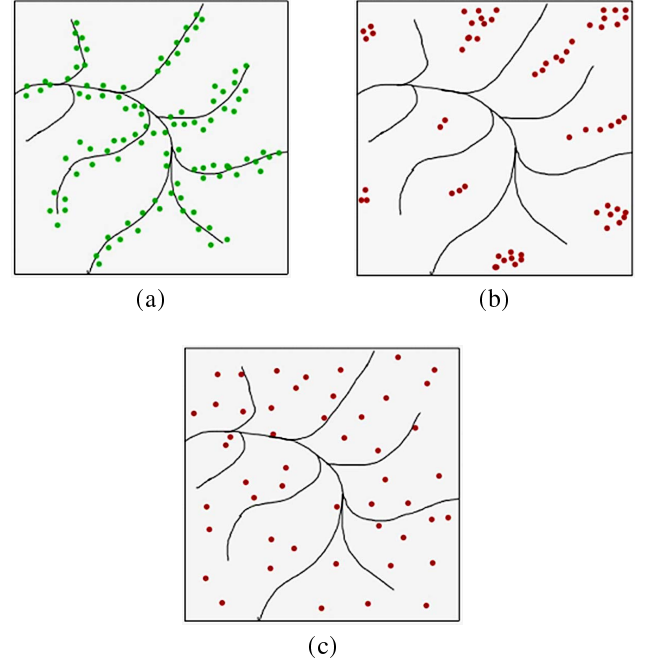


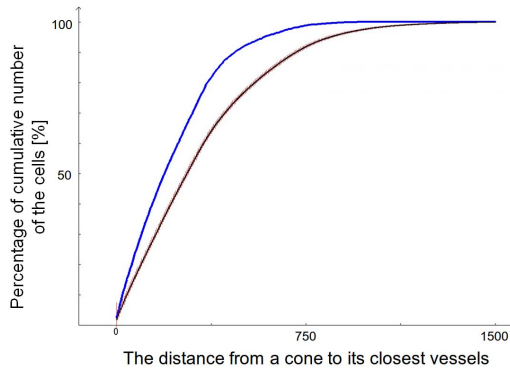
Fig. 3. Three types of the cone distributions in the retina image: (a) positive correlation; (b) negative correlation; and (c) random distribution.

vessels is called the positive correlation distribution (PCD). The negative correlation distribution (NCD) indicates that the cones tend to stay away from the vessels (Fig.3(b)). As illustrated in Fig.3(c), while the cone cells do not have significant correlation with vessels, the cone distribution is regarded as the random distribution (RD).

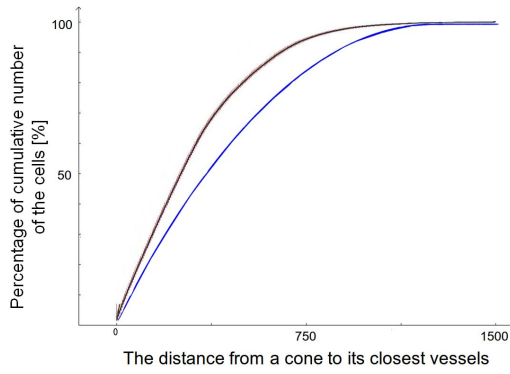
In the case of the PCD, the number of the cells with the small vessel distance is larger than that of the RD. This means that the CFD curve of PCD moves steeply up, and lies above the curve of RD (Fig. 4(a)). On the contrary, as shown in Fig. 4(b), the CFD curve of the NCD is gradually increased, and tend to be located below the curve of the RD. Therefore, the pattern of the cell distribution is identified based on the RD.

To realize this, the CFD curve of the RD is modeled by using virtual retina images. Based on the vessel image, a virtual retina image is generated by selecting as virtual cells randomly from all the pixels except the vessel pixels. The random selection is made by Monte Carlo simulation. For each virtual image, the CFD curve is constructed. Collecting all the CFD curves, the CFD curve model of the RD is described by the distribution with the mean and standard deviation of the curves. Fig. 5 depicts the CFD curve model of the RD obtained from the vessel image (Fig. 7(b)). The square of the enlarged view in the figure shows the mean and standard deviation of the model.

Using the cell and vessel images, the CFD curve H is obtained, and compared with the CFD curve model H_r of the RD. When the CFD curve lies above the upper limit of H_r and not within the standard deviation of H_r , the cell distribution is regarded as the PCD. On the contrary, H is located below H_r and not within the range of the standard deviation, the spatial relationship belongs to the NCD. When H lies in the standard deviation range, there is no significant correlation, that is, the



(a)



(b)

Fig. 4. Comparison of the CFD curves (a) PCD (blue) vs RD (brown); (b) NCD (blue) vs RD (brown).

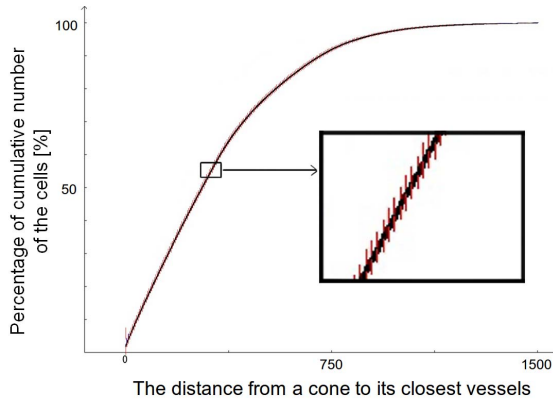
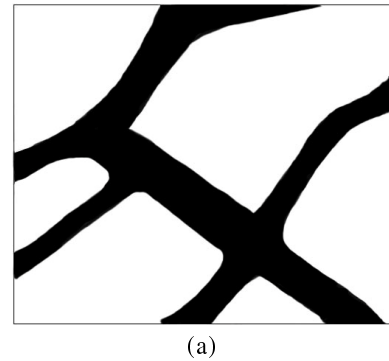


Fig. 5. Cumulative frequency distribution of random cone distributions obtained from the vessel image as shown in Fig. 7(a)

RD.

C. Efficient calculation of vessel distances using a distance map

The high-resolution retina images contain a large number of pixels. For example, the size of the retina images as shown in Fig. 7 (a) used in our method is 3,278 pixels in width and 3,059 pixels in height. Many virtual images with high-resolution are used to construct the CFD curve model H_r of the RD. In the construction, the calculation of the vessel distances



(a)

7	6	5	4	3	2	1	0	0	0	0	0	0	1	2	3	4	4
6	5	4	3	2	1	0	0	1	1	1	2	2	3	4	4	3	2
6	5	4	3	2	1	0	0	1	1	2	2	3	4	4	3	2	2
5	4	3	2	1	0	0	1	1	2	2	3	3	4	4	3	2	1
4	4	3	2	1	0	0	1	2	3	3	4	4	4	3	2	1	0
3	3	2	1	0	0	1	2	3	4	4	5	4	3	2	1	0	0
2	2	1	1	0	0	1	2	3	4	5	4	3	2	1	0	0	1
1	1	0	0	0	1	1	1	2	3	4	3	2	1	0	0	1	2
0	0	0	0	0	0	0	1	2	3	2	1	0	0	1	2	3	2
0	0	1	0	0	0	0	0	1	2	2	1	0	1	2	3	4	4
1	1	1	0	0	1	0	0	0	0	1	1	0	0	1	2	3	4
2	2	1	0	0	1	1	0	0	0	0	1	0	1	2	3	4	5
2	1	0	0	1	2	2	1	0	0	0	0	0	1	2	3	4	5
1	0	0	1	2	3	3	2	1	0	0	0	0	1	2	3	4	5
0	0	1	2	3	4	4	3	2	1	0	0	0	1	2	3	4	5
1	1	2	3	4	4	3	2	1	0	0	0	1	0	0	1	2	3

(b)

Fig. 6. Example of (b) a distance map obtained from (a) a vessel image.

of the cells is time-consuming because the closest vessel pixel of each cell needs to be found from many pixels. Here, since the virtual images are generated based on the vessel image, the locations of the vessel pixels are fixed in all the virtual images. Considering this, a distance map is introduced to speed up the calculation of the vessel distances.

The data structure of the distance map is a 2-D array with the same size of the vessel image. Fig. 6 (b) is the constructed distance map from the vessel image as shown in Fig. 6 (a). In the figure, the black elements correspond to the vessel pixels. To build the distance map, the distance map is initialized by setting all the element to zero. For each pixels except the vessel pixels, its vessels distances are computed, and stored in the element with the same locations of the pixel. The white elements in Fig.6 have the vessels distances of their corresponding pixels.

When the virtual retina image is given, the vessel distance of the cell is obtained by only referring the element with the same locations of the cell. Therefore, the use of the distance map results in the efficient CFD construction.

III. EXPERIMENT

To verify the applicability of the proposed method, we made the experiment using the retina image (Fig. 7 (a)). From the retina image, the cells and the vessels are extracted as shown in Fig. 7 (b) and (c). The retina image contains 4,346 cone cells. Using the vessel image, the virtual retina images are generated by randomly selecting the same number of the pixels

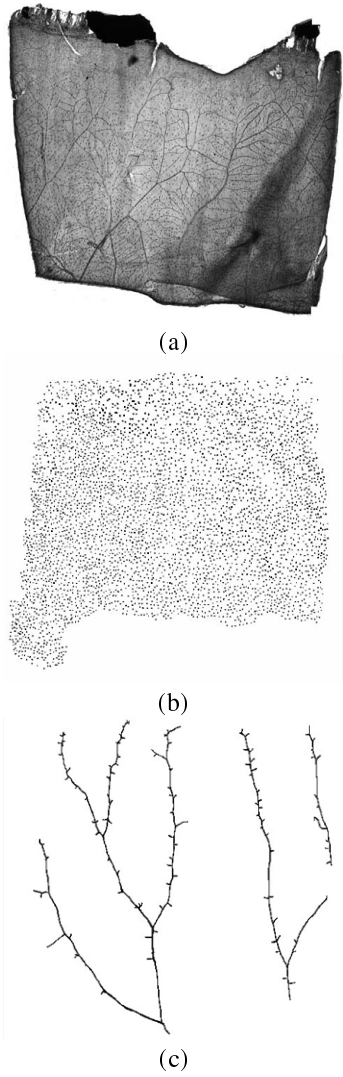


Fig. 7. (a)Retina image used in our experiment, and (b)cones and (c)vessels extracted from the retina image.

as the real cells via Monte Carlo simulation. 5,000 virtual images are generated in the experiment.

We compare two methods for constructing the cumulative frequency distribution: our proposed method using the distance map and the direct method without the distance map. The latter method finds the closest vessel pixels of the virtual cells from the virtual image directly, and computes the vessel distances. Using the 5,000 virtual images, in the direct method, the average computational time of constructing one cumulative frequency distribution is 1.3 [sec] while the construction using the distance map takes 1 [msec]. The proposed method constructs the model H_r of the cumulative frequency distribution curve of the RD (the brown curve in Fig.8). The model construction takes 5 [sec], and our proposed method using the distance map is about 1,300 faster than that of the direct method.

The curve H of the cumulative frequency distribution curve is constructed from the real retina image (the blue curve in Fig. 8). Compared with H_r , the curve H lies above the upper limit of H_r and not within the standard deviation of H_r . Therefore,

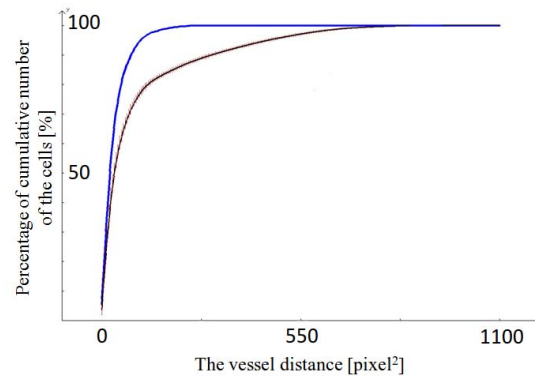


Fig. 8. Cumulative frequency distribution of cones as shown in Fig.7(a)

the cell distribution is identified as the PCD.

IV. CONCLUSION

This paper presents a method for identifying the distribution of cone cells in a given retina image based on the spatial relationship between the cells and vessels. The spatial relationship is represented by the curve of the cumulative frequency distribution of the distances between the cells and their closest blood vessels. Using the curve, the cell distribution is classified into three types: positive correlation, negative correlation, and random distributions.

Our future works include the evaluation of the proposed method by applying to many retina images. In addition, the cone cells and the vessels are manually extracted from retina images. There are methods for tracing blood vessels from retina images[9]. The automatic extraction of both the cone cells and the vessels is one of our future works.

REFERENCES

- [1] J.B. Jonas, J.A. Muller-Bergh, U.M. Schlotter-Schrehardt, G.O. Naumann, "Histomorphometry of human optic nerve", *Investigative Ophthalmology & Visual Science*, vol.31, no.4, pp.736–744, 1990.
- [2] V. Sanguineti, M. Giugliano, M. Grattarola, P. Morasso, "Neuroengineering: from neural interfaces to biological computers", *Communications Through Virtual Technologies*, pp.233–246, 2001.
- [3] C. Morillas, S. Romero, A. Martinez, F. Pelayo, E. Ros, E. Fernandez, "A design framework to model retinas", *Biosystems*, vol.87, issues.2-3, pp.156–163, 2007.
- [4] W. Fink, M.A. Tarbell, "CYCLOPS: A mobile robotic platform for testing and validating image processing and autonomous navigation algorithms in support of artificial vision prostheses", *Computer Methods and Programs in Biomedicine*, vol.96, issue.3, pp.226–233, 2009.
- [5] S. Eglen, "Development of regular cellular spacing in the retina: theoretical models", *Mathematical Medicine and Biology*, vol.23, issue.2, pp.79–99, 2006.
- [6] C.A. Curcio, K.R. Sloan JR, O. Packer, A.E. Hendrickson, R.E. Kalina, "Distribution of Cones in Human and Monkey Retina: Individual Variability and Radial Asymmetry", *Science* 236, pp.579–582, 1987.
- [7] H. Song, T. Yuen, P. Chui, Z. Zhong, A.E. Elsner, S.A. Burns, "Variation of Cone Photoreceptor Packing Density with Retinal Eccentricity and Age", *Investigative Ophthalmology & Visual Science*, vol.52, no.10, pp.7376–7384, 2011.

- [8] H. Song, T. Yuen, P. Chui, Z. Zhong, A.E. Elsner, S.A. Burns, "Variation of Cone Photoreceptor Packing Density with Retinal Eccentricity and Age", *Investigative Ophthalmology & Visual Science*, vol.52, no.10, pp.7376-7384, 2011
- [9] O.M. Mozos, J.A. Bolea, J.M. Fernandez, P.K. Ahnelt, E. Fernandez, "V-Proportion: A Method Based on the Voronoi Diagram to Study Spatial Relations in Neuronal Mosaics of the Retina", *Neurocomputing*, vol.74, issues 1–3, pp.418–427, 2010.
- [9] L. Wang, V. Kallein, M. Bansal, J. Eledath, H. Sawhney, K. Karp, D.J. Pearson, M.D. Mills, G.E. Quinn, R.A. Stone, "Interactive Retinal Vessel Extraction by Integrating Vessel Tracing and Graph Search", *MICCAI 2013, LNCS 8150*, pp.567–574, 2013.